CARBON 54 (2013) 143–148

Available at www.sciencedirect.com

SciVerse ScienceDirect

journal homepage: www.elsevier.com/locate/carbon

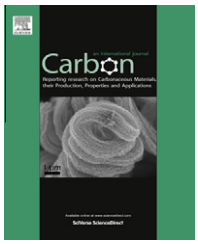

High quality graphene sheets from graphene oxide by hot-pressing

Yupeng Zhang [a], Delong Li [a], Xiaojian Tan [a], Bin Zhang [a], Xuefeng Ruan [a], Huijun Liu [a], Chunxu Pan [a,*], Lei Liao [a,*], Tianyou Zhai [b], Yoshio Bando [b], Shanshan Chen [c], Weiwei Cai [d], Rodney S. Ruoff [c]

[a] School of Physics and Technology, Center for Electron Microscopy and MOE Key Laboratory of Artificial Micro- and Nano-structures, Wuhan University, Wuhan 430072, People's Republic of China

[b] International Center for Young Scientists (ICYS) and International, Center for Materials Nanoarchitectonics (MANA), National Institute for Materials Science (NIMS), Namiki 1-1, Tsukuba, Ibaraki 305-0044, Japan

[c] Department of Mechanical Engineering and The Texas Materials Institute, University of Texas at Austin, One University Station C2200, Austin, TX 78712, USA

[d] Department of Physics Xiamen University, Xiamen 361005, People's Republic of China

ARTICLE INFO

Article history:
Received 24 August 2012
Accepted 7 November 2012
Available online 14 November 2012

ABSTRACT

We report a simple and effective route to convert graphene oxide sheets to good quality graphene sheets using hot pressing. The reduced graphene oxide sheets obtained from graphene oxide by low temperature thermal exfoliation are annealed at 1500 °C and 40 MPa uniaxial pressures for 5 min in vacuum. No appreciable oxygen content was observed from X-ray photoelectron spectroscopy and no D peak was detected in the Raman spectrum. The graphene sheets produced had a much higher electron mobility (1000 $cm^2 V^{-1} S^{-1}$) than other chemically modified graphenes.

1. Introduction

Since its successful isolation by mechanical exfoliation [1,2], graphene has attracted a strong recent interest. It is a promising material for energy-storage, interfacing to biological materials, for electronic and optical devices, and other applications [3,4], due to its unique physical, chemical and mechanical properties, which include high values of Young's modulus (~1100 GPa) [5,6], specific surface area (calculated value, 2630 $m^2 g^{-1}$) [7], thermal conductivity (~5000 $Wm^{-1} K^{-1}$) [8], mobility of charge carriers (exceeding 200,000 cm^2/V s) at room temperature [9], saturation velocity (4.5×10^7 cm/s) [10], and critical current densities (~3×10^9 A/cm^2) [11]. Methods of obtaining C-pure graphene sheets is thus of strategic interest.

A variety of methods exist for synthesizing graphene sheets with either top-down or bottom-up approaches. Graphene or chemically modified graphene can be made from four different methods including mechanical exfoliation, chemical exfoliation, epitaxial growth on SiC and chemical vapor deposition on metal surfaces [12–16]. Mechanical exfoliation, epitaxial growth on SiC, and chemical vapor deposition yield 'C-pure' graphene sheets, which are very useful as attractive electronic materials for further micro- and nano-electronics. However, the relatively small yield and high costs have limited its development in electrodes of lithium ion batteries and supercapacitors, hydrogen storage, composites reinforcement, catalysis, and so on. 'Chemical exfoliation' is employed for 'large scale' (gram-scale and larger) production of 'graphene' sheets. However, the defects and some chemical functional groups such as hydroxyl (C—OH), carboxyl (C=O, O=C—OH), and epoxide group (C—O—C) could be introduced on the graphene sheets inevitably, which alters the physical

* *Corresponding authors*: Fax: +86 27 68752003.
E-mail addresses: cxpan@whu.edu.cn (C. Pan), liaolei@whu.edu.cn (L. Liao).
0008-6223/$ - see front matter
http://dx.doi.org/10.1016/j.carbon.2012.11.012

and chemical properties. It should be noted that so far the reduction of oxygen content in reduced graphene oxide (RGO) is still very difficult [17]. After thermal or chemical treatment, the C═O and O═C—OH could be partially removed or converted to a new chemical species (C—OH), whereas the remaining C—OH or C—O—C in RGO could not be reduced easily, leading to the degradation of electrical properties of the graphene sheets. Scalable conversion of chemically modified graphenes to C-pure graphene sheets still remains a central challenge.

Herein, we report a simple and effective route to convert graphene oxide (GO) sheets to graphene sheets using hot pressing. The product materials were assessed by scanning electron microscopy (SEM), high-resolution transmission electron microscopy (HRTEM), Fourier transform infrared spectroscopy (FT-IR), X-ray photoelectron spectroscopy (XPS) as well as Raman spectroscopy. Significantly, no appreciable oxygen content was observed from XPS, and in the Raman spectrum, no D peak was detected, while the G and 2D peaks characteristic of highly crystalline graphene were readily observed. Moreover, the product graphene sheets had much higher electron mobility (1000 $cm^2 V^{-1} S^{-1}$) than other chemically modified graphenes [18–20]. We believe that, highly crystalline graphene sheets from hot pressing treatment will provide an opportunity and a possibility to radically overcome the barrier for further application of graphene.

2. Experimental

2.1. Materials

Graphite powder, natural, ~325 mesh, 99.95% was purchased from Alfa Aesar. P_2O_5, $K_2S_2O_4$, and $KMnO_4$ with analytical grade and 98% H_2SO_4, 30% H_2O_2 aqueous solution were purchased from Shanghai Chemical Reagents Company, and were used directly without further purification.

2.2. Preparation and thermal reduction of GO

Graphite oxide was synthesized from natural graphite by a modified Hummers method [21]. The product (graphite oxide) was then purified by dialysis to completely remove residual salts and acids. After ultrasonication for 1 h and drying at 60 °C, the graphite oxide was calcined at 700 °C for 2 h under argon atmosphere with a heating rate 100 °C min^{-1} [22].

2.3. Hot pressing treatment of RGO

The product graphene was then treated in a Spark Plasma Sintering (SPS) system (SPS-3.20MK-II, Sumitomo Heavy Industries) under vacuum at 500, 1000, and 1500 °C for 5 min with 0, 5, 10, 20, 30, 40 MPa uniaxial pressures, respectively. The heating rate was 100 °C min^{-1}, and vacuum level was less than 30 Pa. A graphite mold was chosen as the electrode and heating stage.

2.4. Characterization of the samples

The surface morphology of the pristine RGO and the hot pressed graphene sheets were examined by SEM (FEI SIRION) operated at 15 kV. Two kinds of the samples were sonicated in ethanol for 2 h and the suspensions were dropped onto the micro-grid for HRTEM observation (JEOL JEM 2010FEF) at 200 kV. The Atomic Force Microscope (AFM) measurements were performed with a Nanoscope multimode instrument in the air at ambient temperature and pressure. Ethanol suspensions of the graphene sheets were spin-coated onto a SiO_2 (300 nm) substrate, and the solvent was removed by annealing under Ar gas at 600 °C for 1 h. The IR spectrum was measured with a FT-IR spectrometer (Nicolet iS10, Thermo) for detecting the surface functional groups on the samples.

In order to verify the improvement of quality and structural integrity in the hot pressed graphene, chemical compositions and chemical environment of the carbon atoms were measured by using XPS (AXIS-Ultra instrument, Kratos Analytical), with monochromatic Al Kα radiation (225 w, 15 Ma, 15 kV) and low-energy electron flooding for charge compensation.

Raman measurement was carried out using Raman spectroscopy (HORIBA Jobin Yvon LabRAM HR). The power of laser was 15 mW, and the laser excitation was 488 nm. Scans were taken on an extended range (1000–3000 cm^{-1}) and the exposure time was 5 s. Samples were sonicated in ethanol and drop-casted onto a SiO_2 (300 nm) substrate for optic observation.

The electrical transport properties were measured by a Lakeshore probe station (Lakeshore TTPX probe station with Agilent analyser) with home built data acquisition system in ambient condition at room temperature. Toward the electrical characterization, the pristine and hot pressed graphene sheets were first deposited on a highly doped p-type silicon substrate with a 300 nm thick thermal silicon oxide layer, and then contacted by e-beam lithography (JEOL 6510 with NPGS) and metallization process to define the external and drain electrodes. About 20 different sets of samples were tried to verify the reproducibility of the electrical test.

2.5. Theoretical calculations

Molecular dynamics simulation was carried out to understand the structural change of RGO treated by hot pressing. A 0.5 ns step size, constant temperature and constant uniaxial pressures were applied to the molecular dynamics simulation with periodic boundary conditions. The C—C bond was treated with the Tersoff potential while the C—O and O—O were described by a constructed Morse potential fitted from first-principle total energy calculations [23,24].

3. Results and discussion

The conversion process consists of four steps, shown in Fig. 1a. Our novel contribution is that the RGO sheets were then treated by hot pressing at 1500 °C and 40 MPa uniaxial pressures for 5 min in vacuum. The RGO sheets were thereby converted from a pile of powder into a compacted lamellar material with tight combination (see Fig. S1). From the characterizations studies (see Fig. S2), the hot pressing did not change the original morphologies of the RGO sheets (such as size and number of layers), i.e., the RGO sheets did not transform into graphite; this high T, moderate pressure treatment resulted in highly crystalline graphene with a gram-scale output.

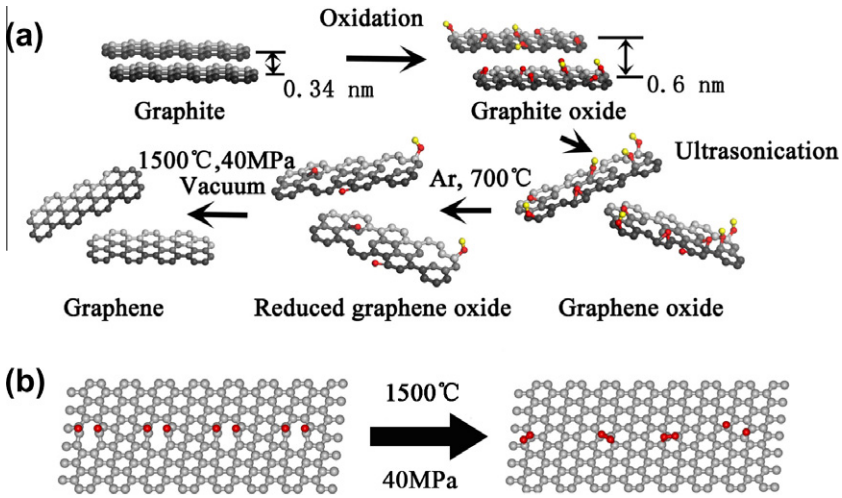

Fig. 1 – (a) Schematic of experimental process to produce high quality graphene sheets from graphene oxide. (b) The initial and final structures of RGO treated by hot pressing during the molecular dynamics simulations.

We have performed molecular dynamics simulations to investigate the structural changes of RGO. Initially, oxygen atoms are chemisorbed on the RGO surface and the underlying C—C bond is broken (Fig. 1b, left). Then, a 0.5 ns step size, constant temperature and constant uniaxial pressures were applied to the molecular dynamics simulation with periodic boundary conditions. Finally, the simulated structure of RGO at a temperature of 1500 °C and pressure of 40 MPa (Fig. 1b, right) showed that the honeycomb structure of graphene was recovered through the formation of C—C and O—O bonds.

SEM images of the product graphene sheets showed well exfoliated graphene sheets (Fig. 2a). TEM imaging revealed less wrinkles and foldings in product sheets, and the dark lines at the edge of the sheets were straightened (Fig. 2b). Comparatively, a large number of intrinsic wrinkles were formed, due to the existing of atom group, and the dark lines were curved in RGO sheets (see Fig. S3). These changes indicated that the defects and residual chemical functional groups in RGO sheets have been removed completely during hot pressing treatment. Further electron diffraction and atomic imaging of the product sheets by TEM showed the crystalline structure of graphene, which also proved the high quality of the treated graphene. AFM image of the product sheets transferred onto a SiO_2 (300 nm-thick thermal oxide) substrate by spin-coating (Fig. 2c) showed a thickness of approximately 0.9 nm, namely, single-layer graphene (Fig. 2d).

FTIR and XPS showed a strong reduction in functional groups in the product sheets (Fig. 3) [25–28]. According to the XPS survey spectrum, the RGO sheets and the treated graphene sheets contained only elements carbon (C) and oxygen (O) with chemical binding energies of C1s (284.7 eV) and O1s (532.0 eV). Obviously, the oxygen content in the treated graphene sheets was much less than that in the RGO. The C1s XPS spectrum revealed that the hydroxyl groups (C—OH) and carbonyl groups (C=O) in RGO have vanished, and a sharp peak at 284.7 eV shows the presence of sp^2 hybridized carbon atoms. The spectroscopy suggested the total or near total removal of O-containing functional groups by the hot pressing step.

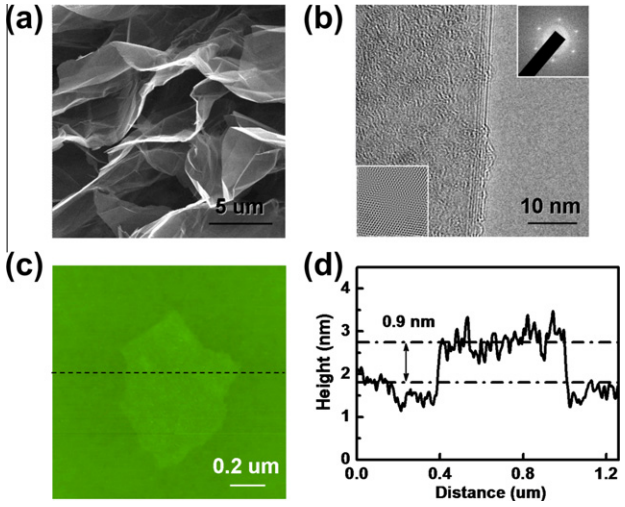

Fig. 2 – Characterizations of the product graphene sheets treated by hot pressing. (a) SEM image shows an existence of well exfoliated graphene sheets. (b) HRTEM image of the product sheet edge with fast Fourier transform (FFT) and inverse-FEF map insert. (c and d) AFM image and its height profile showing a flake with a height of 0.9 nm.

Raman spectroscopy is an easy and effective approach to evaluate the crystalline quality and the number of stacking layers of graphene sheets by monitoring the relative intensity of the D peak (defect-related) and the G peak (doubly degenerate zone center E_{2g} mode) [29–31]. The G and 2D peaks are indicative of graphene or graphitic carbon, while the D peak indicates 'defects' (functionalized carbon atoms, point defects, etc.). The I_D/I_G ratio has been used as a measure of the degree of crystallization or surface defects density of graphene [32].

In order to further understand the important role of the temperature and the pressure in the process, Raman spectroscopy was done on samples treated at different conditions.

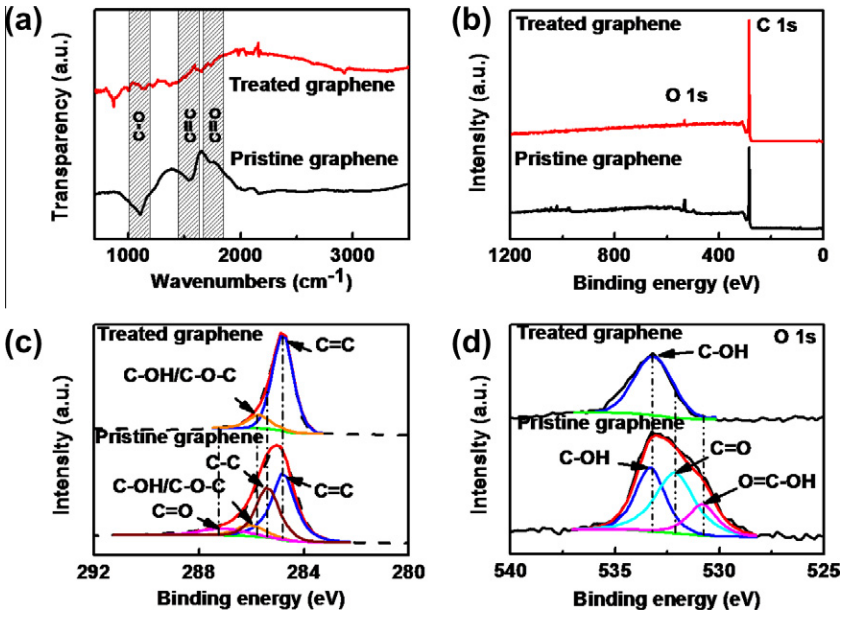

Fig. 3 – (a) FT-IR spectra (400–3500 cm^{-1}) of the RGO and hot pressed graphene sheets with shaded regions representing signal of functional groups. (b) XPS survey scan spectrum of the RGO and hot pressed graphene sheets. (c) C1s spectral region. (d) O1s spectral region.

With T fixed at 1500 °C, the D peak intensity started to decrease with the applied pressure increased and the intensity of the 2D peak was recovered (Figs. 4a and b). At 40 MPa, the D peak has disappeared, showing that defects and functional groups have been removed from the RGO sheets and that the sp^2 carbon network has been entirely reconstructed. With pressure fixed at 40 MPa, the D/G intensity ratio decreased as the temperature was increased. At 1500 °C, the D peak was eliminated (Fig. 4c). The G/2D intensity ratio and the Full Width Half Maximum (FWHM) of 2D peak imply that the sample consisted of monolayer, bilayer and few layer of graphene (Fig. 4d). On the basis of statistical sampling of the treated graphene sheets using Raman and AFM, it was estimated that 80% of the product (graphene) sheets were less than five layers.

We note that at temperatures between 1000 and 2000 °C and the indicated pressures, single layer or few layer graphene

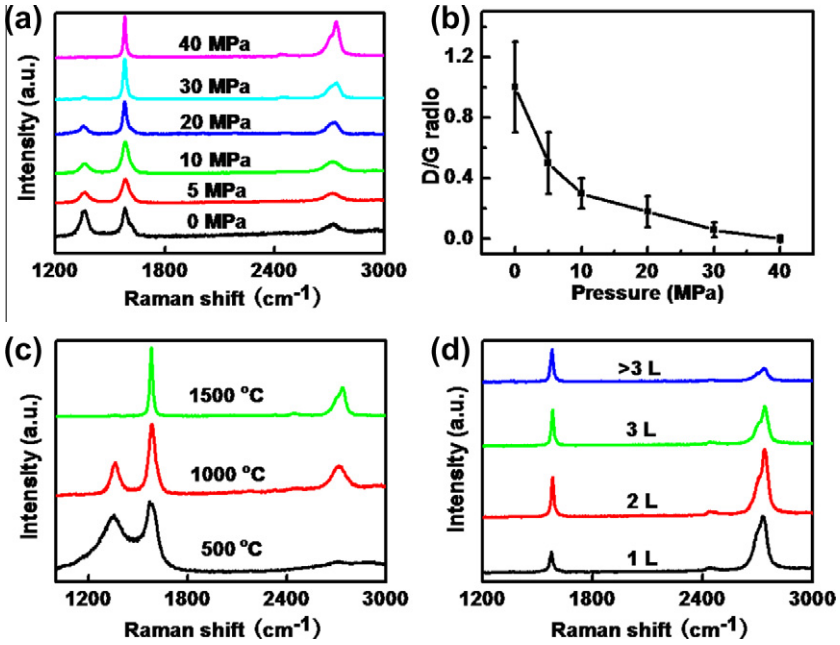

Fig. 4 – Characterizations of the hot pressed graphene sheets using Raman spectroscopy. (a) Raman spectra of hot pressed graphene as a function of the pressure at 1500 °C. (b) D/G ration of hot pressed graphene as a function of the pressure at 1500 °C. (c) Raman spectra of hot pressed graphene as a function of the temperature at 40 MPa pressure. (d) Raman spectra of hot pressed graphene with variant layers.

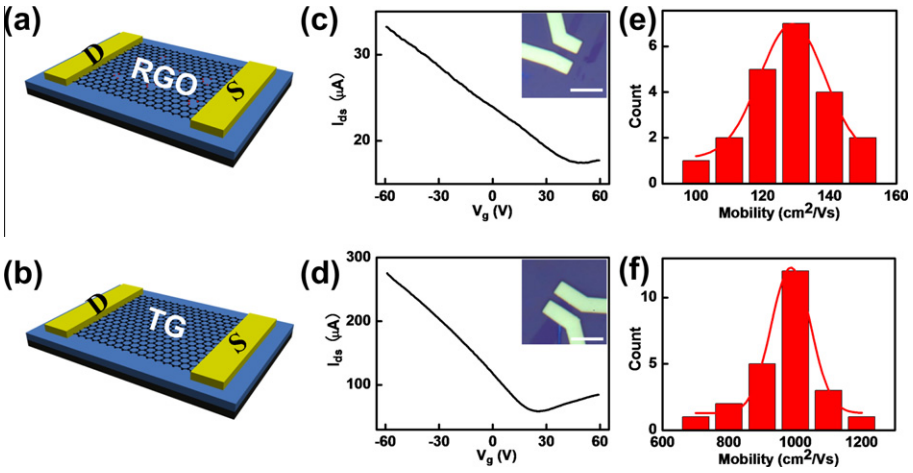

Fig. 5 – The electrical properties of the RGO and the hot pressed graphene sheet transistor. (a and b) The schematic top view of the device layout. D, drain; S, source; RGO, reduced graphene oxide; TG, treated graphene by hot pressing. (c and d) I_{ds}–V_g transfer characterize for the RGO and treated graphene transistor at V_{ds} = 0.1 V, inset in (c) and (d) are optical images of the transistor device, the scale bar is 5 μm. The external source and drain are fabricated using electron beam lithography. (e and f) Mobility distribution maps of RGO and treated graphene.

was obtained. However, when T is raised above 2400 °C, the original RGO sheets transformed into bulk graphite. With T about 1500 °C, functional groups on the precursor RGO sheets were apparently completely removed. The application of pressure during high T treatment plays a critical role in obtaining 'high quality' graphene sheets as a product material.

Based on the molecular dynamics simulation data, XPS spectrum results, and the change of vacuum level during hot pressing (Fig. S4), the mechanism of reducing functional groups through hot-pressing could be thoroughly discussed. The above results indicated that the reaction was divided into two stages, first stage primarily is the C═O and O═C—OH bonds decomposition at 800–1500 °C. Subsequently, when the pressure was fixed at 40 MPa, the C—OH and C—O—C bonds started to be removed due to the formation of C—C and O—O bonds, which resulted in the recovery of the honeycomb structure of graphene.

Field effect transistors (FETs) from pristine RGO sheets and also of the high (T, p) treated RGO sheets were fabricated on a 300 nm SiO_2/Si substrate [33,34]. The schematic top views of a FET composed of RGO or of the product sheet, as the channel, with source and drain electrode, and back gate, are shown in Fig. 5a and b, respectively. Fig. 5c and d shows the current I as a function of the applied gate voltage V_g, where the conduction carrier is hole for a positive V_g. The average mobility was about 1000 $cm^2\ V^{-1}\ S^{-1}$ for the product (graphene) sheets (about 8× higher than the RGO precursor sheets, where the RGO sheets show a mobility of about 130 $cm^2\ V^{-1}\ S^{-1}$) (Fig. 5e and f). Moreover, this value exceeds most of the RGO prepared by the chemical reduction method. High reproducibility of the electrical test was verified from the columnar distribution map and the Gauss distribution curve.

4. Summary

The perfectly structural integrity and gram-scale production of graphene have been physically produced using hot pressing with high temperature and moderate pressure. The process is simple and effective, meeting the industrial level requirement of graphene applications. Besides the chemical produced graphene sheets, the graphene sheets from other processes may also be treated with hot pressing for further getting a perfect and highly crystalline graphene. This process could provide a possibility to radically overcome the barrier for further industrial use of graphene with low-cost in energy and composites in the future.

Acknowledgements

This research was supported by the National Natural Science Foundation of China (No. 11174227), National Basic Research Program of China (973 Program) (No. 2009CB939705), academic award for excellent Ph.D. candidates funded by Ministry of Education of China, and the Fundamental Research Fund for the Central Universities (2011202020003). L. Liao acknowledges the MOE NCET-10-0643 and NSFC Grant (Nos. 11104207, 91123009 and 10975109), Hubei Province Natural Science Foundation (2011CDB271), the Natural Science of Jiangsu Grant (No. BK2011348), as well as "The Grant of State Key Laboratory of Advanced Technology for Materials Synthesis and Processing (Wuhan University of Technology)". The authors acknowledge the helpful input of D. Zhao, Y. Ren, Q. Fu, D. Wang, Y. Liu and W. Yao. XPS measurements were carried out at the Analysis Center, Tsinghua University. AFM measurements were carried out at the School of Materials Science and Engineering, Wuhan University of Technology

Appendix A. Supplementary material

Supplementary data associated with this article can be found, in the online version, at http://dx.doi.org/10.1016/j.carbon.2012.11.012.

REFERENCES

[1] Novoselov KS, Geim AK, Morozov SV, Jiang D, Katsnelson MI, Grigorieva IV, et al. Two-dimensional gas of massless dirac fermions in graphene. Nature 2005;438(10):197–200.
[2] Novoselov KS, Geim AK, Morozov SV, Jiang D, Zhang Y, Dubonos SV, et al. Electric field effect in atomically thin carbon films. Science 2004;306(5696):666–9.
[3] Stankovich S, Dikin DA, Dommett GHB, Kohlhaas KM, Zimney EJ, Stach EA, et al. Graphene-based composite materials. Nature 2006;442(7100):282–6.
[4] Rao CNR, Sood AK, Subrahmanyam KS, Govindaraj A. Graphene: the new two-dimensional nanomaterial. Angew Chem Int Ed 2009;48(42):7752–77.
[5] Zhang Y, Pan C. Measurements of mechanical properties and number of layers of graphene from nano-indentation. Diam Relat Mater 2012;24:1–5.
[6] Lee C, Wei X, Kysar JW, Hone J. Measurement of the elastic properties and intrinsic strength of monolayer graphene. Science 2008;321(5887):385–8.
[7] Stoller MD, Park S, Zhu Y, An J, Ruoff RS. Graphene-based ultracapacitors. Nano Lett 2008;8(10):3498–502.
[8] Balandin AA, Ghosh S, Bao W, Calizo I, Teweldebrhan D, Miao F, et al. Superior thermal conductivity of single-layer graphene. Nano Lett 2008;8(3):902–7.
[9] Bolotin KI, Sikes KJ, Jiang Z, Klima M, Fudenberg G, Hone J, et al. Ultrahigh electron mobility in suspended graphene. Solid State Commun 2008;146(9):351–5.
[10] Neugebauer P, Orlita M, Faugeras C, Barra AL, Potemski M. How perfect can graphene be? Phys Rev Lett 2009;103(13):136403.
[11] Du X, Skachko I, Barker A, Andrei EY. Approaching ballistic transport in suspended graphene. Nat Nanotechnol 2008;3(8):491–5.
[12] Novoselov KS, Jiang D, Schedin F, Booth TJ, Khotkevich VV, Morozov SV, et al. Two-dimensional atomic crystals. Proc Natl Acad Sci USA 2005;102(30):10451–3.
[13] Shriram S, Barton RA, Yu X, Alden J, Hermen L, Chandrashekhar MVS, et al. Free-standing epitaxial graphene. Nano Lett 2009;9(9):3100–5.
[14] Li X, Cai W, An J, Kim S, Nah J, Yang D, et al. Large-area synthesis of high-quality and uniform graphene films on copper foils. Science 2009;324(5932):1312–4.
[15] Zhu Y, Murali S, Cai W, Li X, Suk JW, Potts JR, et al. Graphene and graphene oxide: synthesis, properties, and applications. Adv Mater 2010;22(35):3906–24.
[16] Rao CNR, Subrahmanyam KS, Ramakrishna Matte HSS, Abdulhakeem B, Govindaraj A, Das B, et al. A study of the synthetic methods and properties of graphenes. Sci Technol Adv Mater 2010;11(5):054502.
[17] Yang D, Velamakanni A, Bozoklu G, Park S, Stoller M, Piner RD, et al. Chemical analysis of graphene oxide films after heat and chemical treatments by X-ray photoelecton and micro-Raman spectroscropy. Carbon 2009;47(1):145–52.
[18] Chen W, Yan L, Bangal PR. Preparation of graphene by the rapid and mild thermal reduction of graphene oxide induced by microwaves. Carbon 2010;48(4):1146–52.
[19] Stankovich S, Dikin DA, Piner RD, Kohlhaas KA, Kleinhammes A, Jia Y, et al. Synthesis of graphene-based nanosheets via chemical reduction of exfoliated graphite oxide. Carbon 2007;45(7):1558–65.
[20] Wang J, Manga KK, Bao Q, Loh KP. High-yield synthesis of few-layer graphene flakes through electrochemical expansion of graphite in propylene carbonate electrolyte. J Am Chem Soc 2011;133(23):8888–91.
[21] Kovtyukhova NI, Ollivier PJ, Martin BR, Mallouk TE, Chizhik SA, Buzaneva EV, et al. Layer-by-layer assembly of ultrathin composite films from micron-dized graphite oxide sheets and polycations. Chem Mater 1999;11(3):771–8.
[22] Mcallister MJ, Li JL, Adamson DH, Schniepp HC, Abdala AA, Liu J, et al. Single sheet functionalized graphene by oxidation and thermal expansion of graphite. Chem Mater 2007;19(18):4396–404.
[23] Tewary VK, Yang B. Parametric interatomic potential for graphene. Phys Rev B 2009;79(7):075442.
[24] Belytschko T, Xiao SP, Schatz GC, Ruoff RS. Atomistic simulations of nanotube fracture. Phys Rev B 2002;65(23):235430.
[25] Si Y, Samulski ET. Synthesis of water soluble graphene. Nano Lett 2008;8(6):1679–82.
[26] Li X, Zhang G, Bai X, Sun X, Wang X, Wang E, et al. Highly conducting graphene sheets and langmuir–blodgett films. Nat Nanotechnol 2008;3(9):538–42.
[27] Campos-Delgado J, Romo-Herrera JM, Jia X, Cullen DA, Muramatsu H, Kim YA, et al. Bulk production of a new form of sp^2 carbon: crystalline graphene nanoribbons. Nano Lett 2008;8(9):2773–8.
[28] Choucair M, Thordarson P, Stride JA. Gram-scale production of graphene based on solvothermal synthesis and sonication. Nat Nanotechnol 2009;4(1):30–3.
[29] Ferrari AC, Meyer JC, Scardaci V, Casiraghi C, Lazzeri M, Mauri F, et al. Raman spectrum of graphene and graphene layers. Phys Rev Lett 2006;97(18):187401.
[30] Ferrari AC. Raman spectroscopy of graphene and graphite: disorder, electron–phonon coupling, doping and nonadiabatic effects. Solid State Commun 2007;143(1):47–57.
[31] Gao L, Ren W, Li F, Cheng HM. Total color difference for rapid and accurate identification of graphene. ACS Nano 2008;2(8):1625–33.
[32] Cancado LG, Jorio A, Martins Ferreira EH, Stavale F, Achete CA, Capaz RB, et al. Quantifying defects in graphene via raman spectroscopy at different excitation energies. Nano Lett 2011;11(8):3190–6.
[33] Liao L, Bai JW, Cheng R, Lin YC, Jiang S, Huang Y, et al. Top-gated graphene nanoribbon transistors with ultrathin high-k dielectrics. Nano Lett 2010;10(5):1917–21.
[34] Liao L, Bai JW, Cheng R, Lin YC, Jiang S, Qu Q, et al. Sub-100 nm channel length graphene transistors. Nano Lett 2010;10(10):3952–6.